# Feasibility of Separation Processes in Liquid-Liquid Solid Systems: Free Energy and Stability Analysis

MALCOLM T. JACQUES
A. DAVID HOVARONGKURA
and
JOSEPH D. HENRY, JR.

Department of Chemical Engineering
West Virginia University
Morgantown, West Virginia 26506

The feasibility of new solid/liquid separation processes, such as solids removal from oil and certain tertiary oil recovery techniques, can be evaluated by a thermodynamic stability analysis of possible liquid-liquid-particle configurations. The thermodynamic stability and hence feasibility of two possible liquid-liquid-particle separation process is predicted by use of a free energy analysis. Stability is shown to depend primarily on droplet/particle size ratio $(n)$ and three phase contact angle $(\theta)$. Stability criteria are presented which can be applied to many particle and liquid separation processes.

## SCOPE

The stability of liquid-liquid-particle systems is of considerable concern in many chemical and energy process applications. Several solids separation processes, for example, rely on the distribution of suspended particles from a bulk liquid phase into a second immiscible liquid phase which is then subsequently separated from the bulk phase prior to removal of the particulates. Examples of such applications include particle removal from oil continuous media using an aqueous solution as the second immiscible liquid and selective removal of cell particles and macromolecules from body fluids by use of a second immiscible liquid.

Other separation processes utilize a second immiscible liquid to form a bridge between suspended particles resulting in particle agglomeration prior to removal of the solids. Examples of this type of separation process are found in tar sand treatment to remove suspended solids. Selective agglomeration and fractionation techniques are also used for the beneficiation of low grade coals and ores.

An increasingly important process area in which the interactions between two immiscible liquids and solid particles play an important role is in the removal of a liquid phase from the interstices of a densely packed particle matrix. Several tertiary oil recovery techniques, such as surfactant or micellar flooding, utilize a bulk aqueous phase to remove the immiscible oil phase from the interstices of the oil bearing strata.

Despite the widespread application and growing demand of new energy based processes for liquid-liquid-particle separations, there is surprisingly little fundamental information available on the mechanisms and parameters which govern such systems. Consequently, a systematic evaluation of possible liquid-liquid-particle separation techniques for new process applications cannot be accomplished without expensive and time consuming trial and error experimentation.

This paper attempts to partially redress these shortcomings and presents a general thermodynamic surface-energy analysis, the results of which are used to infer the relative stability of possible liquid-liquid-particle configurations of interest in separation process applications.

The free energy of an initial equilibrium state consisting of single discrete spherical particles and immiscible liquid droplets dispersed in a bulk liquid phase is evaluated in terms of dispersed droplet/particle size ratio $(n)$, three phase contact angle $(\theta)$, and liquid-liquid surface tension $(\gamma_{23})$. Two possible final equilibrium states are then considered, in which either single particles are distributed into the dispersed liquid droplets or two particles are bridged by a single dispersed droplet. The difference in free energy between these possible initial and final equilibrium states is then used to deduce which is the most stable configuration. The equilibrium state with the lowest free energy is assumed to be the most stable.

These two final equilibrium states are used to illustrate the use of a free energy stability analysis for two alternate separation processes, namely, particle distribution from a bulk liquid phase into a distributed liquid phase and particle agglomeration or bridging by means of a second immiscible liquid. It is important to recognize that the data presented in this paper are specific to the two liquid-liquid-particle configurations considered. It is possible that other configurations exist which possess a lower free energy and are consequently more stable and hence more likely to be encountered in practice than the configurations analyzed in this paper. However, the free energy stability analysis has general applicability to any liquid-liquid-particle configuration.

The analysis presented here clearly reveals whether or not a particular liquid-liquid-particle separation process, such as agglomeration, is possible for a given system in terms of the specific three phase contact angle $(\theta)$ and dispersed droplet/particle size ratio $(n)$ of that system. If the specific values of these governing parameters do not fall within the predicted ranges for thermodynamic stability, the separation process under consideration is unlikely to be feasible. Techniques are available for the accurate measurement of $\theta$, $n$, and $\gamma_{23}$, thereby permitting a quantitative evaluation of the feasibility of specific separation processes without recourse to complicated and tedious chemical screening techniques currently employed in many separation process evaluation studies.

# CONCLUSIONS AND SIGNIFICANCE

The feasibility of two possible liquid-liquid-particle separation processes is examined in terms of suspension stability by application of a free energy analysis. For each case, the range of three phase contact angle ($\theta$), necessary for a successful separation, is predicted for any range of dispersed droplet/particle size ratio ($n$). The first type of separation process considered represents distribution of suspended particles into a second, immiscible, dispersed liquid phase. It is shown that in systems where the particles are preferentially wetted by the dispersed liquid phase, the three phase contact angle must be within the range $0 \leqslant \theta < \pi/2$ for distribution to occur. More specifically, for given values of dispersed droplet/particle size ratio ($n$), critical values of $\theta$ are predicted, below which distribution may occur and above which it may not. The most stable equilibrium state is shown to be obtained when $\theta \to 0$ and $n \to \infty$, corresponding to small three phase contact angles and large dispersed droplet size.

The second separation process considered in this paper relies on the formation of a liquid bridge between at least two particles as a result of encounter with a dispersed droplet. This process forms the basis for several separation processes including spherical agglomeration and selective agglomeration used in tar sand extract treatment and coal beneficiation processes, respectively. The range of the three phase contact angle ($\theta$) required for thermodynamic stability of the liquid bridge is predicted by a free energy analysis for any possible dispersed droplet/particle size ratio ($n$). It is shown that for particles preferentially wetted by the dispersed phase, bridging is only possible when $0 \leqslant \theta < \pi/2$, and that a definite limit on the range of $\theta$ exists for each value of $n$. This limiting value of $\theta$ is shown to decrease as $n$ increases, and the most thermodynamically stable bridges are formed for small $\theta$ and large $n$, that is, large droplets.

The major significance of this work is that a deeper understanding of the parameters and mechanisms controlling the stability of liquid-liquid-particle systems has been obtained. In addition, the results of the analytical model presented enables the feasibility of any proposed liquid-liquid-particle separation process to be evaluated without recourse to qualitative experimental investigation. The most significant applications of this work are believed to be in the assessment of new liquid-liquid-particle separation processes, where only a limited data base on necessary parameter values exists. Such new process areas include particle removal from coal derived liquids; particle removal from shale oil, tar sand, and pyrolysis oil extracts; and low grade coal and ore beneficiation processes. One other very important area which involves the reverse process outlined in this paper lies in the tertiary oil recovery field. Here a second immiscible bulk liquid is used to displace the oil from the oil bearing particle matrix. The stability analysis presented here can readily be applied to this type of separation process by simply reversing the initial and final equilibrium states and considering a closely packed particle system.

The information obtained from this stability analysis can provide a useful starting point and frame of reference for the assessment of a new separation process. It is important to realize that the stability analysis predicts only whether or not the desired end state is thermodynamically stable at equilibrium. Several other stability considerations must be taken into account for specific processes. These must include the effects on stability of such factors as shear, mixing, temperature, surface absorption characteristics, dissolution, and solubility kinetics, all of which will vary considerably from process to process. In addition, other liquid-liquid-particle configurations are possible which could have lower free energies and hence be more stable than either of the two configurations analyzed in this paper.

---

The chemical and energy industries employ numerous processes which utilize the physical and chemical interactions between two immiscible liquid phases and solid particles. The science and technology involved in such processes spans a considerable range in both complexity and understanding, varying from sophisticated electrochemical theories of colloid science to some of the more pragmatic applications of solids separation technology. Attempts to unify the somewhat diverse subject matter and applications in this field have resulted in several excellent reviews of the available literature.

Mizrahi and Barnea (1972) produced a comprehensive review on this subject in which they identified seven different fields where liquid-liquid-particle interactions play a major role in the overall process. These seven fields fall broadly into two distinct categories. The first involves the influence of particles on the forma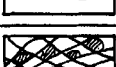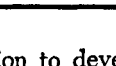tion and coalescence of liquid dispersions, including the important subject of solids stabilized emulsions. The second category includes some of the less conventional solids separation techniques which include separation of solids by liquid-liquid extraction, the use of a second liquid phase to enhance heavy liquid sink-float separations, differential flotation for ultrafine particles, mixing and separations in liquid-liquid-particle systems in which the particles are either produced or consumed by chemical reaction, and the agglomeration and separation of solids from liquid suspensions by the spherical agglomeration process.

Almost all conventional solids separation processes, and most of the aforementioned less conventional processes, have been developed for solids removal from aqueous phases. However, with the current interest in new energy related processes such as coal liquefaction, tertiary oil recovery, in-situ retorting of oil shales, and oil recovery from tar sands, there is an urgent need to develop novel processes for the separation of solids from nonaqueous media.

One such process which is already finding application in the recovery of crude oil from tar sands is the spherical agglomeration process. Puddington and Sparks (1975) have reviewed some of the fundamentals and applications of this process which utilizes bridging between individual particles by a second liquid phase that preferentially wets the suspended particles and ultimately results in the formation of large, dense, spherical agglomerates. This proc-

TABLE 1. CLASSIFICATION AND SCHEMATIC REPRESENTATION
OF SOME LIQUID-LIQUID-PARTICLE SEPARATION PROCESSES

| Basis of Liquid-Liquid-Particle Separation Process. | Process Applications and Examples | Schematic Representation of Change in Liquid-Liquid-Particle Relationship During Separation Process. | Change in State Corresponding to Convention of Figures 1 & 2 |
|---|---|---|---|
| Particle Distribution Between Two Liquid Phases. | Particle removal from oil continuous phase e.g., ash removal from coal derived liquids (Henry et.al. 1976, Prudich 1978.) | | I ⟶ II |
| | Emulsion breaking by use of particulates e.g., oil in water emulsion breaking using glass powder(Mizrahi 1970) | | II ⟶ I |
| | Partitioning of cell particles and macromolecules (Albertsson 1971) e.g., selective removal of red blood cells from contaminated blood plasma. | | I ⟶ II |
| Pariticle separation from Continuous Liquid Phase by Bridging with a Dispersed Liquid Phase. | Particle agglomeration and separation by settling e.g., solids removal from tar sand oil (Puddington 1975). | | III ⟶ IV |
| | Selective agglomeration of solids fractionation e.g., coal beneficiation (Capes 1970) | | III ⟶ IV |
| | Enhancement of heavy liquid sink float separations by use of second liquid e.g. iron or quartz separation (Mizrahi 1972) | | III ⟶ IV |
| Separation of Bridging Liquid from Dense Particle Matrix by Use of a Second Continuous Liquid Phase. | Tertiary oil recovery e.g., surfactant flooding. | | IV ⟶ III |
| | Leaching, e.g., minimization of liquid entrainment in gangue. | | IV ⟶ III |
| | De-inking of wood pulp fibers e.g., deinking of newsprint. | | IV ⟶ III |
| | Impregnation of fiber matrix with second liquid phase e.g., fire retardant of fiber board. | | IV ⟶ IV |

ess has found extensive use in the mining and chemical industries for the separation of finely divided solids from liquid suspensions. It is singled out here because of its significance to the understanding of liquid-liquid-particle interactions and because of its potential application to nonaqueous systems.

The significance of liquid-liquid-particle separation processes in the fields of fossil energy recovery and processing is further emphasized in the review of Capes (1976) who discusses basic research in particle technology and some novel applications. Here, again, the spherical agglomeration process is emphasized because of its applications in the beneficiation of coal fines and the upgrading of waste materials.

The processes mentioned above have been the subject of considerable research and development, and there now exists a large body of literature and a good understanding of the process parameters which influence macroscopic characteristics, such as agglomerate size and strength of the liquid-liquid-particle interactions. However, a generalized theory dealing with the microscopic interfacial interactions, common to all liquid-liquid-particle processes, is still not available. Mizrahi and Barnea (1972) attempted to initiate an effort to unify the available information in this area, ranging from entirely empirical to theoretical thermodynamic analyses, into a generalized theoretical picture. The purpose of this paper is to extend their effort and also to identify new areas of technological importance pertaining to liquid-liquid-particle separation processes.

One such area is the removal of residual particulates from the reactor effluent stream of several proposed coal liquefaction processes. Henry et al. (1976) and Prudich and Henry (1978) are currently actively involved in an investigation to develop a process for the distribution of these particulates from the coal derived liquid into an aqueous phase. Conventional, and less costly, aqueous phase solids separation processes can then be employed to recover the solids.

Similar solids removal problems from nonaqueous liquids occur in the treating of some crude oils, though the quantity of solids present is much smaller than in the case of coal derived liquids. Oil obtained from in-situ retorting of oil shales presents another process which also requires a solids removal step before acceptable product quality can be obtained, as does the oil recovered from pyrolysis of municipal refuse. Each of these areas represent possible candidates for the use of a process employing a second immiscible liquid phase as a likely technique for effecting particle removal from the oil phase.

All the aforementioned applications of the various liquid-liquid-particle separation processes are summarized in Table 1, where the process applications are classified into three groups according to the basis of the separation process. Specific examples of each process application are cited together with references. The changes in the relationships between the liquid and solid phases are shown schematically for each process application, together with the state change in accordance with the nomenclature of Figures 1 and 2.

The processes mentioned so far, corresponding to the first and second classification on the basis of the separation process in Table 1, have as their major objective either the separation of particulates from a liquid phase by the use of a second liquid phase or the separation of two liquid phases by the use of solid particles. A third and increasingly important class of processes involves the
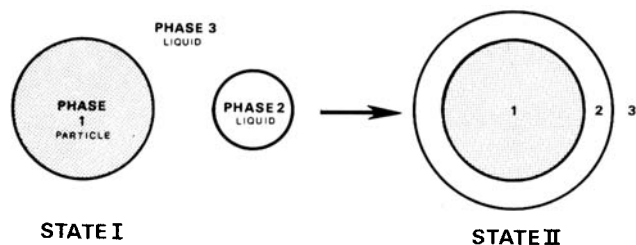
**Fig. 1. Process of particle (phase 1) distribution from continuous liquid phase 3 into dispersed liquid phase 2, showing phase relationship between initial state I and final state II configurations.**
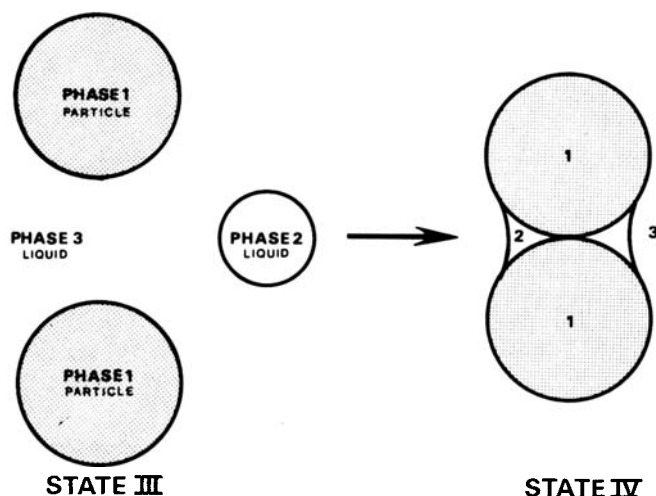


**Fig. 2. Process of liquid bridge formation showing phase relationship between initial state III and final state IV configurations.**

separation of one liquid phase from a bulk solid phase by the use of a second liquid phase. This corresponds to the third classification in Table 1. Crude oil recovery from tar sands by the use of alkaline solutions, Doscher (1977), and in-situ tertiary oil recovery methods using surfactant or micellar flooding techniques fall into this third class of liquid separations from solids. Both tar sands and many types of oil bearing strata, Moody (1961), can be considered to consist of discrete close packed particles surrounded by a continuous oil or water phase. Other oil bearing strata are considered to consist of a continuous porous spongelike solid matrix with a continuous oil or water phase contained in the capillaries. In either case, the microscopic characteristics of the liquid-liquid-solid interface are similar, and the only significant difference between these structures is the capillary forces holding the liquid phases either in the porous or interstitial solid matrix. However, because of the more general applicability to the several processes mentioned previously, this paper will only address the behavior of discrete particles in a liquid-liquid dispersion.

Separations of liquid-liquid-particle mixtures have as a basis of operation one physical process common to almost all different techniques. This common process consists essentially of changing the free energy of the system in order to effect the desired separation between phases. The simplest example of this, in the case of particle distribution from one liquid phase into another, is that of a single particle being transferred by gravity across a planar interface between the liquid phases. This transfer can be viewed simply from a thermodynamic standpoint in which only the initial and final free energy states are considered. Such an analysis reveals important information on whether or not the desired separation is thermodynamically feasible. Information on the path or force needed to surmount

the energy barrier which the particle may experience is more readily obtained via a free body analysis of the dynamics of a particle at a liquid-liquid interface.

The force balance on a single particle at a horizontal interface has received considerable attention, owing primarily to its significance in flotation theory. Princen (1969) details the free body force analysis on such systems and presents analytical solutions for the minimum cylindrical and prismatic particle size which can attain equilibrium at a fluid-fluid interface. Rapachietta and Neumann (1977) carry this analysis further and solve the force balance equation for spherical particles. In addition, they present a generalized thermodynamic approach, based on a free energy analysis, which complements and confirms the results of the force balance approach. Both analyses show that the important variables in the system are the three phase contact angle, particle geometry, and density differences.

## ANALYTICAL MODELS

This paper presents a generalized thermodynamic analysis of only two possible states which spherical particles can take in a liquid-liquid dispersion. The analysis is applied only to two possible initial and desired final states of the system from a separation point of view. System parameters such as three phase contact angle needed to effect the desired separation are evaluated. The free energy approach is completely general and can be applied to any possible liquid-liquid-particle configuration in addition to the two outlined in this paper. Further, the stability of processes involving both particle separation from liquid dispersion and liquid separation from a particle matrix can be analyzed by this method. Consequently, the analysis provides meaningful information for most of the processes given in Table 1.

One important variable in many practical separation processes is the relative sizes and size distributions of the particle and liquid dispersions. The size variables are incorporated in the free energy analysis in the form of a ratio of droplet to particle radii. The results of this analysis show that careful control of the size variable can greatly enhance or retard the separation process. In addition, a force-balance analysis for a spherical particle at a curved interface is presented which corroborates the free energy analysis results.

### FREE ENERGY ANALYSIS OF LIQUID-LIQUID-PARTICLE SYSTEMS

Consider a spherical particle 1 of radius $r_1$, initially suspended in a continuous liquid phase 3, in which there is also dispersed droplets of a second immiscible liquid 2 of radius $r_2$, as shown in Figure 1, state I. (The liquid droplet is shown smaller than the particle to be consistent with the nomenclature for the bridging analysis. In many process applications, the liquid droplet will, of course, be larger than the particle.) Assume that the desired final state of this system, from a separation viewpoint, is complete wetting or distribution of the particle into the dispersed liquid phase, as shown in Figure 1, state II. It is also quite possible that in some practical applications the reverse process, that is, II → I, may be the desired separation.

The actual conditions, in terms of particle dynamics, necessary to effect either of the above two separations can be inferred from a free body force analysis which is discussed more fully later in this paper.

Interaction between the dispersed liquid and particle phases can lead to an alternative end state if two or more particles are considered. Figure 2 shows the alterna-

tive initial and final end states for the formation of a liquid bridge between two spherical particles. Here again, this fundamental step is common to several separation processes. Figure 2 can be considered to represent the initial stages in the formation of a solid flocculant or agglomerate, which may subsequently be separated by conventional sedimentation techniques, or further agglomeration can be induced as in the spherical agglomeration process, Puddington and Sparks (1975). The reverse process to that shown in Figure 2 can be considered as a possible basic process in the separation of oil from porous media, as discussed earlier, and depicted in Table 1.

The thermodynamic stability of the alternative final states depicted in Figures 1 and 2 can be obtained by a free energy analysis, the most stable state being that with the lowest free energy and the most likely change being that associated with a negative free energy difference.

The free energy difference of the changes in state depicted in Figures 1 and 2 can be determined as follows:

$$F_I = 4\pi r_1^2 \gamma_{13} + 4\pi r_2^2 \gamma_{23} \qquad (1)$$

$$\text{let} \quad n = r_2/r_1 \qquad (2)$$

Defining $F_I'$ as the free-energy per unit surface area of the particle, we get

$$F_I' = \gamma_{13} + n^2 \gamma_{23} \qquad (3)$$

Similarly, for state II

$$F_{II} = 4\pi r_1^2 \gamma_{12} + 4\pi \bar{r}_2^2 \gamma_{23} \qquad (4)$$

and

$$\bar{r}_2 = (r_1^3 + r_2^3)^{1/3} \qquad (5)$$

Substituting for $r_2$ in (5) from (2), we get

$$\bar{r}_2 = r_1 (1 + n^3)^{1/3} \qquad (6)$$

$$F'_{II} = \gamma_{12} + (1 + n^3)^{2/3} \gamma_{23} \qquad (7)$$

From Figure 2, the free energy of state III is given by

$$F_{III} = 8\pi r_1^2 \gamma_{13} + 4\pi r_2^2 \gamma_{23} \qquad (8)$$

that is

$$F'_{III} = 2\gamma_{13} + n^2 \gamma_{23} \qquad (9)$$
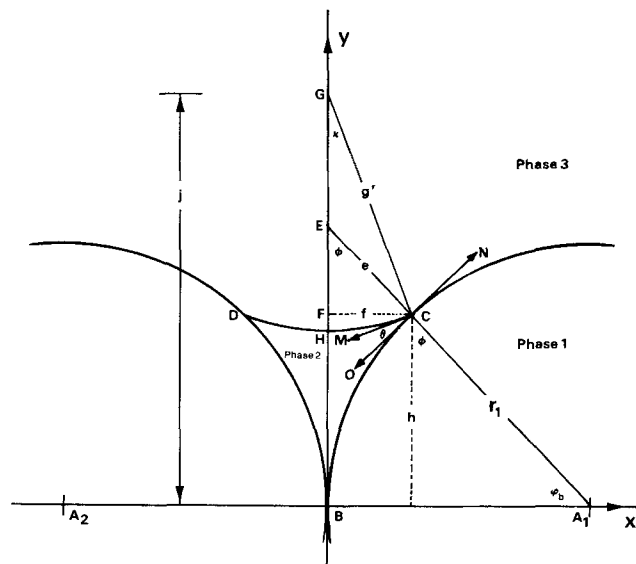
The free energy of state IV is given by



Fig. 3. Detail of liquid bridge geometry, assuming circular profile (see appendix).

$F_{IV} = $ (Surface area of 23 interface). $\gamma_{23}$
$\qquad + 2$ (Surface area of 12 interface per particle) $\gamma_{12}$
$\qquad + 2$ (Surface area of 13 interface per particle) $\gamma_{13}$

$$\qquad (10)$$

The surface area of the 23 interfaces is defined uniquely by the geometry assumed by the bridging liquid. The liquid bridge can adopt one of several possible geometries which result in the 23 interface, having a profile which is that of a segment of either a circle, nodoid, catenoid, or unduloid. Figure 3 shows details of the interfacial geometry assuming the 23 surface profile to be circular. Figure 4 shows a photograph of two glass beads bridged by water. It can be seen that DC is an arc of a circle which has a radius of GC. The detailed analysis of the liquid bridge geometry is presented in the appendix. This analysis enables the area of the 23 interface to be defined uniquely in terms of a single geometric parameter $\psi_b$ (see Figure 3) for a given contact angle $\theta$.

From the appendix



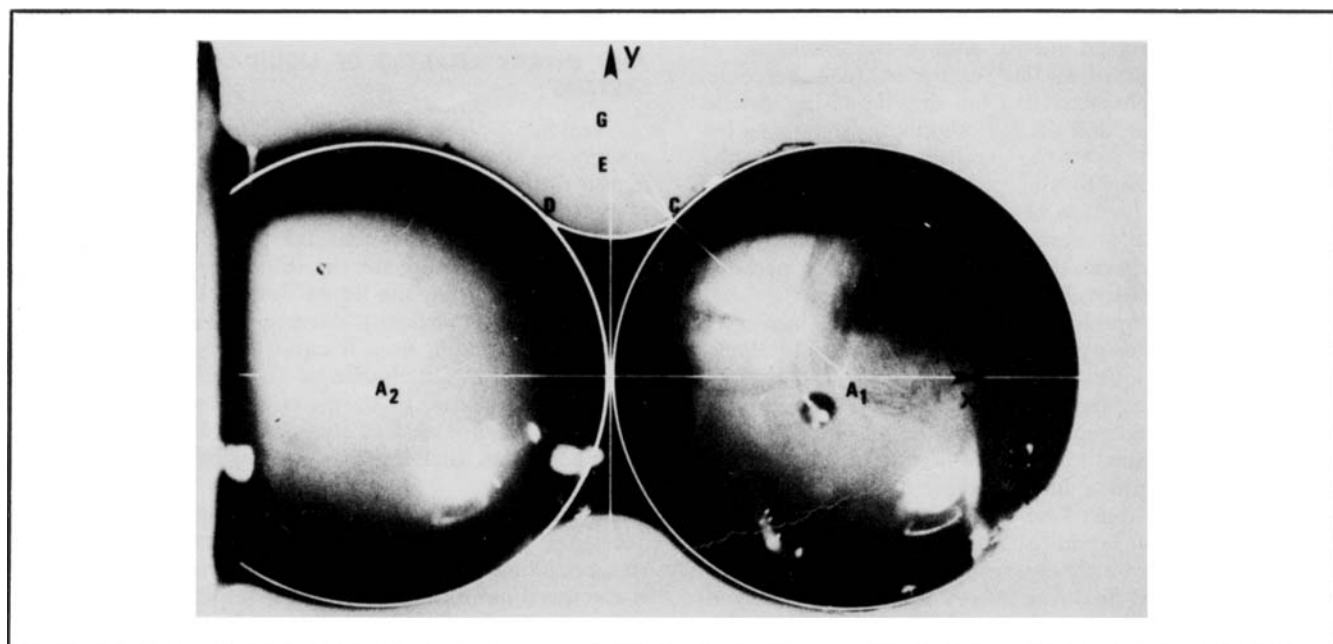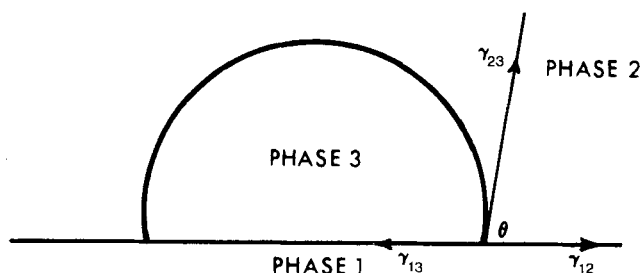Fig. 4. A photograph of two spherical glass beads bridged by water.

Fig. 5. Diagram illustrating the definition of the three phase contact angle $\theta$. Solid phase 1 preferentially wetted by continuous liquid phase 2; that is, $\theta > \pi/2$.
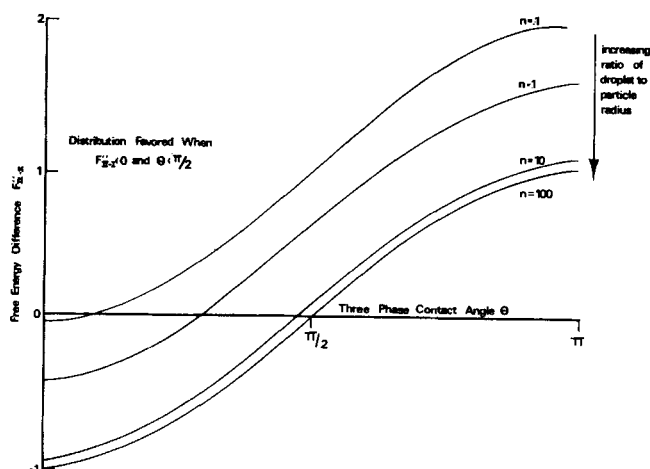


Fig. 6. Difference in free energy between states II and I showing significance of $\theta$ and $n$ when the particle is preferentially wetted by phase 2 liquid.

Surface area of 23 interface $= 4\pi r_1^2 F_1(\psi_b, \theta)$   (11)

Surface area of 12 interface/particle $= 2\pi r_1^2 (1 - \cos \psi_b)$

(12)

Surface area of 13 interface/particle $= 4\pi r_1^2$

$- 2\pi r_1^2 (1 - \cos \psi_b)$   (13)

Substituting Equations (11), (12), and (13) into (10), we get the free energy per unit area of solid particle as

$F'_{IV} = \gamma_{23} F_1(\psi_b, \theta) - (1 - \cos \psi_b)\gamma_{23} \cos \theta + 2\gamma_{13}$

(14)

The preferred thermodynamic states of the liquid-liquid-particle systems shown in Figures 1 and 2 can be inferred by calculating the differences in free energy from Equations (3), (7), (9), and (14).

The difference in free energy between states II and I is given by

$F'_{II} - F'_I = (\gamma_{12} - \gamma_{13}) + \gamma_{23} [(1 + n^3)^{2/3} - n^2]$

(15)

The relationship between the three phase contact angle $\theta$ and the surface tension forces $\gamma_{12}$, $\gamma_{13}$, and $\gamma_{23}$ is given by Young's equation

$\gamma_{13} - \gamma_{12} = \gamma_{23} \cos\theta$   (16)

where $\theta$ is measured through phase 2 as shown in Figure 5, and it is assumed that the solid is preferentially wetted by phase 2 liquid.

Substituting Equation (16) in (15), we get

$F'_{II-I} = \gamma_{23} [(1 + n^3)^{2/3} - n^2 - \cos\theta]$   (17)

Nondimensionalizing the free energy change by $\gamma_{23}$, we get

$F''_{II-I} = [(1 + n^3)^{2/3} - n^2] - \cos\theta$   (18)

The limiting values of $n$ which are physically realizable are $\infty \geqq n \geqq 0$. If $n \to 0$, $F''_{II\to I} \geqq 0$ for all values of $\theta$; hence state II is thermodynamically unstable. However, if $n \to \infty$, $F''_{II\to I} \to - \cos\theta$. Hence, in this case, state II is the lowest free energy condition when $0 < \theta < \pi/2$, and, conversely, when $\pi/2 < \theta < \pi$, state I is the most stable condition.

Similarly, the free energy difference between states IV and III is given by

$F''_{IV-III} = F_1(\psi_b, \theta) - \cos \theta (1 - \cos \psi_b) - n^2$

(19)

In order to solve Equation (19), it is necessary to evaluate $\psi_b$ for given values of $n$ and $\theta$. This is possible, since the volume of the bridging liquid $V_b$ must equal that of the original phase 2 liquid droplet as depicted in Figure 2; that is

$$\frac{4}{3} \pi r_2^3 = 2\pi r_1^3 F_2(\psi_b, \theta)$$   (20)

$$\frac{2}{3} n^3 = F_2(\psi_b, \theta)$$   (21)

Hence, from Equation (21), it can be seen that a unique value of $\psi_b$ exists for given $n$ and $\theta$, which must satisfy the limiting geometrical conditions that $\theta < \pi/2$ and $(\psi_{b, max} + \theta) \leqq \pi/2$. The unique values of $\psi_b$ and $\theta$ obtained by solving Equation (21) can be substituted into Equation (19) to determine the free energy difference between state IV and III.

Equation (19) is, however, limited by the values of $n$, $\psi_b$, and $\theta$ which are imposed by both the geometry of the system and the fact that the analysis presented so far is only valid when phase 2 liquid wets the solid phase 1; that is, $\theta \leqq \pi/2$. If we assume that the liquid bridge cannot extend beyond the equatorial plane of the solid spheres, then $0 < \psi_b < \pi/2$, and from solid geometry $n \leqq (1/2)^{1/3}$. In addition, the geometrical limits on (21) must also be satisfied; that is, $(\psi_{b, max} + \theta) \leqq \pi/2$.

Consequently, (19) can be solved, with the above limits, for given $n$ and $\theta$ and to determine which state has the lowest free energy and is consequently the most stable from a thermodynamic standpoint.
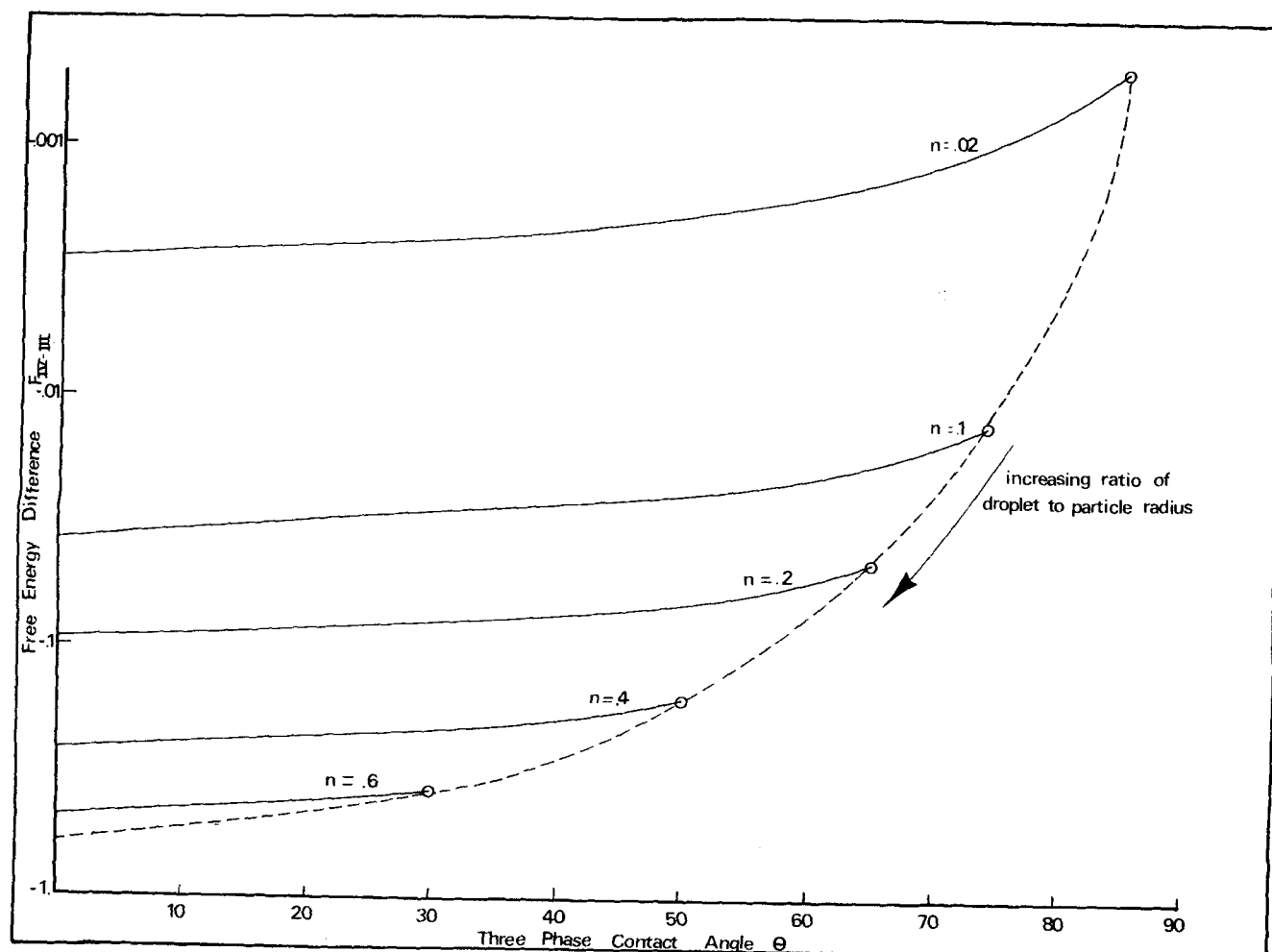
## DISCUSSION OF FREE ENERGY ANALYSIS RESULTS

Figures 6 and 8 show the computed values of $F''_{II\to I}$ and $F''_{IV\to III}$ as functions of $\theta$ and $n$ for a system in which the particles are preferentially wetted by phase 2. It can be seen from Figure 6 that $F''_{II\to I}$ is only negative, for any value of $n$, when $\theta < \pi/2$. Since the preferred thermodynamic state is that with the lowest free energy, which by convention is a negative quantity, it can be inferred that state II will be the most stable state when $\theta < \pi/2$ and $n \to \infty$. In practical terms, this implies that solid particles preferentially wetted by the dispersed phase 2 can be distributed from the continuous liquid phase 3 into droplets of the distributed liquid phase. Also, distribution will be favored by large droplets, that is, $n \to \infty$, and small three phase contact angle, that is, $\theta < \pi/2$.

It can be seen from Figure 6 that for every value of $n$ there exists a critical three phase contact angle $\theta_{crit}$ below which the free energy of state II is less than that of state I. Those critical contact angles are the values of $\theta$ at

**Fig. 7. Variation of critical value of three phase contact angle $\theta_{crit}$ with size parameter n.**
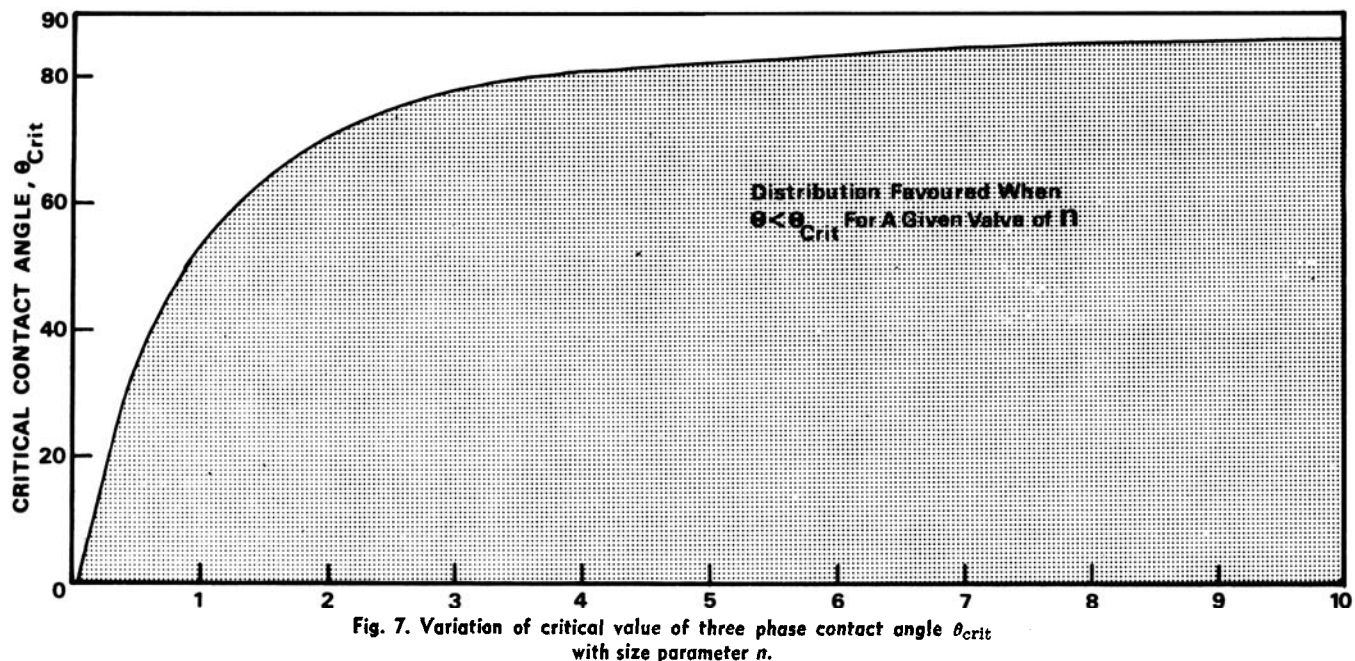
which the $F''_{II \to I}$ curves intersect the $\theta$ axis. Figure 7 shows the critical contact angle as a function of $n$, and it is clear that if $\theta \to \pi/2$, distribution will only be possible for large $n$, that is, large droplets.

Figure 8 shows the computed values of $F''_{IV \to III}$ as functions of $\theta$ and $n$ for a system in which the particles are preferentially wetted by phase 2 liquid. It can be seen that in order for bridging to occur, $\theta < \pi/2$. In addition,
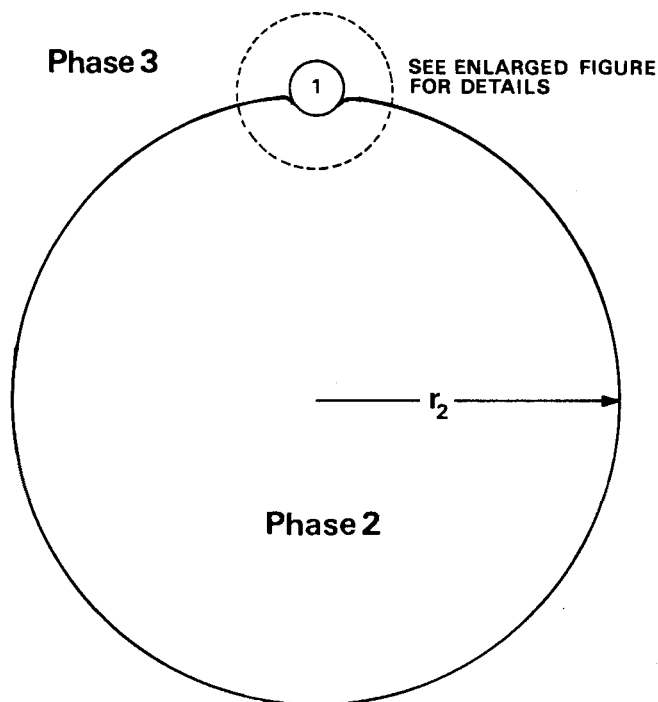


**Fig. 8. Difference in free energy between states IV and III showing significance of $\theta$ and n when the particles are preferentially wetted by phase 2 liquid.**

**Fig. 9. Particle at equilibrium in the interface between a phase 2 droplet and a continuous liquid phase 3.**
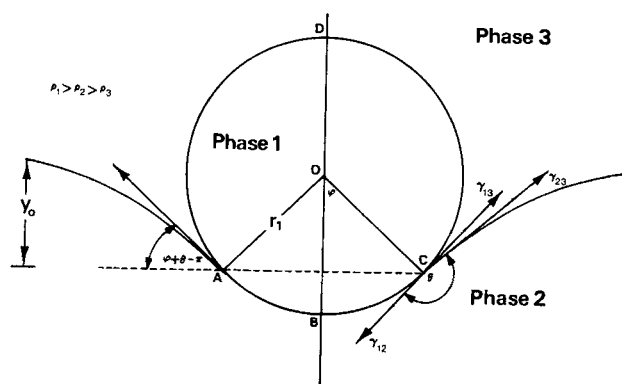


**Fig. 10. Detail of spherical particle, radius $r_1$, embedded in the interface between a droplet, radius $r_2$, of phase 2 liquid, and a continuous liquid phase 3.**

for each value of $n$ there exists a limited range of $\theta$ over which the bridged state IV has the lowest free energy. Furthermore, it can be seen that $F''_{\text{IV}\to\text{III}}$ approaches a minimum as $n$ approaches the limiting value of $(0.5)^{1/3}$, which indicates that the most stable bridges are formed with the largest droplets. However, the limits on the contact angle are much more severe for larger $n$ as can be seen from the $n = 0.6$ curve where the contact angle is bounded by 0 and 30 deg. It is worth reemphasizing that the strongest bridges will be those formed by the larger droplets and low three phase contact angles, since these conditions give the lowest free energy conditions. The above analysis on bridging provides information only on whether or not the bridged state is thermodynamically stable. In order to determine if a bridge will, in fact, form and remain intact in a real process stream, it is necessary to estimate the hydrodynamic and mechanical forces acting on the particles.

One other significant point which arises from this free energy analysis is that the difference in free energy per unit surface area of the solid particles is always

smaller (that is, more negative) for the bridging process than for the distribution process, that is, $F''_{\text{IV}\to\text{III}} < F''_{\text{II}\to\text{I}}$, with $n < (0.5)^{1/3}$. This indicates that bridging is the preferred thermodynamic state and will be more stable than the distributed state.

As previously mentioned, the free energy analysis indicates only the preferred thermodynamic states of the liquid-liquid-particle systems considered in this paper. Information on whether it is possible or even practical to attempt to attain these states can be evaluated by a force balance analysis on a single particle at a liquid-liquid interface. It is, of course, also possible that alternative liquid-liquid-particle configurations, other than the two considered in this paper, have a lower free energy and would consequently be the most stable. To determine which alternative configuration is the most stable is beyond the scope of this paper, but it is clear that a free energy analysis of all possible configurations will reveal the most stable state.

## FORCE BALANCE ANALYSIS

Consider a spherical particle 1 at equilibrium in the interface of a droplet of phase 2 liquid distributed in a continuous liquid phase 3 as shown in Figure 9. Princen (1969) and Rapacchietta and Neumann (1977) have presented detailed analyses for particles at planar interfaces. This analysis differs only in that a curved interface is included.

Figure 10 is a detailed representation of a spherical particle embedded in a liquid-liquid interface, showing the geometrical conventions adopted in the following analysis.

The vertical forces acting on the particle are

$F_1$ = Component of surface tension force at the three phase contact point $(C)$
$F_2$ = Gravitational forces (buoyancy)
$F_3$ = Hydrostatic pressure forces

$$F_1 = 2\pi r_1 \sin \psi\{\gamma_{23} [\sin (\psi + \theta)]\} \qquad (22)$$

$$F_2 = (\text{Volume ABCD})\rho_1 g - (\text{Volume ABC})\rho_2 g$$
$$- (\text{Volume ADC})\rho_3 g$$

and since

$$(\text{Volume ADC}) = (\text{Volume ABCD}) - (\text{Volume ABC})$$

$$F_2 = (\text{Volume ABCD})(\rho_1 - \rho_3)g$$
$$- (\text{Volume ABC})(\rho_2 - \rho_3)g \qquad (23)$$

For a curved liquid-liquid bulk interface, the hydrostatic pressure is determined by the principal radii of curvature. However, if the bulk liquid-liquid interface constitutes a discrete droplet, the hydrostatic pressure within the droplet is everywhere constant and given by Young's equation as

$$p_2 - p_3 = \frac{2\gamma_{32}}{r_2}$$

$$F_3 = (p_2 - p_3)\pi r_1^2 \sin^2\psi \qquad (24)$$

$$F_3 = \frac{2\gamma_{23}}{r_2} \cdot \pi r_1^2 \sin^2\psi$$

At equilibrium $F_1 + F_2 + F_3 = 0$, that is

$$2\pi r_1 \sin \psi\{\gamma_{23} \sin (\psi + \theta)\} + \frac{2\gamma_{23}}{r_2} \pi r_1^2 \sin^2\psi$$

$$= (\text{Volume ABCD})(\rho_1 - \rho_3)g$$
$$- (\text{Volume ABC})(\rho_2 - \rho_3)g$$

Substituting for ABCD and ABC, we get

$$\gamma_{23} \sin \psi \left[ \sin (\psi + \theta) + \frac{r_1}{r_2} \sin \psi \right]$$

$$= \frac{2}{3} r_1^2 (\rho_1 - \rho_3)g - \frac{r_1^2}{6} (1 - \cos \psi)^2$$

$$(2 + \cos \psi)(\rho_2 - \rho_3)g \qquad (25)$$

if the particle is small in comparison to the droplet; that is, if $r_2 \gg r_1$, terms in $r_1^2$ can be neglected, which is equivalent to assuming that to a first approximation gravitational forces are negligible if $r_2 \gg r_1$:

$$\gamma_{23} \sin \psi \left[ \sin(\psi + \theta) + \frac{r_1}{r_2} \sin \psi \right] \simeq 0 \qquad (26)$$

Inspection of Equation (26) shows that there are three possible stable positions for the particle: $\psi = 0$ or $\pi$, which corresponds to the particle completely wetted by phase 3 or phase 2 liquid, respectively, or if $r_1/r_2 \to 0$, $\psi + \theta = \pi$, which corresponds to a stable position in the interface.

Equation (26) can be used to deduce the conditions necessary for the particle to transfer into phase 2 liquid, since in the absence of gravitational forces it is necessary for the surface tension forces to be greater than the hydrostatic forces if the particle is to move further into phase 2; that is, $F_1 > F_3$:

$$\sin(\psi + \theta) > \frac{r_1}{r_2} \sin \psi \qquad (27)$$

Further, if it is assumed that $\psi = \pi/2$, that is, the particle is exactly halfway through the liquid-liquid interface, then by expansion of Equation (27)

$$\cos\theta > r_1/r_2$$

and since $r_1/r_2$ must be finite and positive, it can be seen that the particle cannot distribute into phase 2 liquid, in the absence of gravitational forces, unless $0 < \theta < \pi/2$.

This inference from the force-balance analysis is in exact agreement with that obtained from the free energy analysis; that is, the general condition for a particle, preferentially wetted by phase 2 liquid, to be distributed from a continuous phase 3 liquid into a dispersed phase 2 droplet, is $(0 < \theta < \pi/2)$.

## CONCLUSION

The conditions for a minimum free energy state in two possible particle-liquid-liquid configurations has been determined in terms of three fundamental system parameters, that is, three phase contact angle, the surface tension of the liquid-liquid interface, and the ratio of the dispersed liquid droplet radius to the particle radius. The minimum free energy conditions have been interpreted as probable stable conditions.

The thermodynamic stability assumption has been used to predict the process conditions necessary for three separate classes of liquid-liquid-particle separation processes. The first class comprises of processes in which the objective is to transfer particles from a continuous liquid phase to a second dispersed liquid phase. This separation process corresponds to the distribution of particles from a continuous liquid phase to a dispersed liquid phase.

Applications of the particle distribution process have been identified in Table 1, and particular emphasis is placed on the suitability of this process to the problem of particle removal from a continuous oil phase. The authors are currently investigating such a process for the removal of ash from coal derived liquids. It is felt that similar processes could play an important role as economically viable processes for the removal of solids from some of the newer sources of liquid fuels including shale oil, tar sand oils, and liquid pyrolysis products from municipal solid wastes.

The analysis presented in this paper also predicts the precise range of parameter values needed to affect the reverse process in which particles are added to a liquid-liquid dispersion to cause separation of the liquid phases. This process could prove economically competitive in emulsion breaking processes which currently use high voltage electrostatic coalescers.

A second liquid-liquid-particle separation class has been identified which employs the formation of a liquid bridge between particles to produce larger agglomerates. The free energy analysis applied to this process again shows the important system variables to be three phase contact angle, size ratio of bridging liquid droplets to particles, and liquid-liquid surface tension. Precise values and limits of these variables are evaluated to indicate the process conditions needed for bridging to occur. This process has already found widespread application in the fossil fuel and mineral processing industries. The specific techniques of spherical agglomeration are being utilized to separate solids from tar sand extracts and for coal beneficiation.

The third liquid-liquid-particle separation class corresponds to the reverse process of liquid bridge formation. The removal of oil bridges formed between adjacent particles in oil wet strata constitutes the basis of several tertiary oil recovery techniques. In particular, the surfactant flooding aims at displacing the oil bridges from between particles by use of a continuous aqueous phase containing surfactants. The analysis presented in this paper clearly identifies the conditions necessary to effect removal of the oil bridges in terms of three phase contact angle, liquid droplet to particle size ratio, and liquid-liquid surface tension. This information could prove invaluable in such oil recovery processes, since predictions of the effect the surfactant must have on the above parameters can be made a priori, and simple laboratory experiments can be carried out to evaluate suitable surfactants.

It should of course, be realized that in all three liquid-liquid-particle separation process classifications discussed above, the necessary values of three phase contact angles, droplet to particle size ratio, and liquidi-liqiuid surface tensions are predicted only by a thermodynamic stability analysis. While the results do give considerable insight into the necessary process conditions, no consideration is taken of the effects of practical process conditions such as shear induced by flow and mixing, adsorption and dissolution kinetics of surfactant (that is, mechanism by which surfactant actually reduces three phase contact angle), and/or liquid-liquid surface tension. These various process conditions will vary considerably between different applications and processes. However, the fundamental conclusions about the stability of various states, determined from the free energy analysis, are valid for any liquid-liquid-particle system.

## NOTATION

$A_{12}$ = surface area of 12 interface bridging case
$A_{13}$ = surface area of 13 interface bridging case
$A_b$ = surface area of bridging liquid
$F_1$ = surface tension force at the three phase contact point
$F_2$ = gravitational forces
$F_3$ = hydrostatic pressure forces
$F_I$ = free energy of state I
$F_{II}$ = free energy of state II
$F_{III}$ = free energy of state III
$F_{IV}$ = free energy of state IV
$F'_I$ = free energy per unit solid surface area of state I
$F'_{II}$ = free energy per unit solid surface area of state II
$F'_{III}$ = free energy per unit solid surface area of state III
$F'_{IV}$ = free energy per unit solid surface area of state IV
$F''_{II-I}$ = nondimensionalized change in free energy from state II to I
$F''_{IV-III}$ = nondimensionalized change in free energy from state IV to III
$F_1(\psi_b, \theta)$ = bridging liquid area function
$F_2(\psi_b, \theta)$ = bridging liquid volume function
$f$ = geometry in Figure 3
$g$ = gravitational constant
$g'$ = geometry in Figure 3
$h$ = geometry in Figure 3
$j$ = geometry in Figure 3
$n$ = radii ratio of phase 2 to phase 1
$p_2$ = internal pressure of phase 2
$p_3$ = internal pressure of phase 3
$r_1$ = radius of phase 1
$r_2$ = radius of phase 2
$V_b$ = volume of liquid bridge
$x$ = $x$ coordinate in Figure 3
$y$ = $y$ coordinate in Figure 3

### Greek Letters

$\gamma_{12}$ = surface tension of phase 1 and 2
$\gamma_{13}$ = surface tension of phase 1 and 3
$\gamma_{23}$ = surface tension of phase 2 and 3
$\theta$ = three phase contact angle
$\kappa$ = angle in Figure 3
$\rho_1$ = density of phase 1
$\rho_2$ = density of phase 2
$\rho_3$ = density of phase 3
$\psi$ = angle in Figure 10
$\psi_b$ = filling angle for bridging case, Figure 3

## APPENDIX

Determination of the profile assumed by a liquid bridge formed between two equal spherical particles has received considerable attention because of the significance of such systems to many processes, for example, porosimetry, oil recovery, particle agglomeration, and capillary condensation. Erle et al. (1971) considered the general case for the stability of such liquid bridges between small equal spherical particles. A general expression is presented for the volume occupied by the bridging liquid when the spherical particles remain in contact or are separated by a small distance. Erle et al. (1971) identify mathematical criteria which specify which of the possible geometries the interface assumes. However, a solution to these general area and volume expressions requires numerical integration of Euler-Lagrangian types of equations and a closed form solution exists only for the case of a catenoidal profile. Melrose (1966) also details an exact geometrical theory for such interfaces and presents numerical solutions for the area and volume of a liquid bridge having a nodoidal profile.

However, the free energy analysis presented in this paper utilizes the area and volume of a liquid bridge evaluated assuming that the spherical particles are in contact, and the profile of the bridge is an arc of a circle. This circular assumption greatly simplifies the analysis and has been shown (Hotta et al., 1974; Mayer and Stowe, 1966; Melrose and Wallick, 1967) to result in maximum errors in the computed area and volume of the order of 1%. This approximation yields progressively more accurate results as the bridging volume decreases, since then the circular profile closely approaches that of the more accurate anticlastic nodoidal surface (Melrose and Wallick, 1967).

The area and volume of the bridging liquid, needed to evaluate Equation (10), can be determined by considering Figure 3. The equation of the bridging liquid profile is assumed to be that of circular arc CH and is given by the following analysis and nomenclature of Mayer and Stowe (1966):

$$x^2 + (y - j)^2 = g'^2 \qquad (A1)$$

The surface area of the bridging liquid is given by

$$A_b = 2 \times 2\pi \int_0^\kappa y\, g'\, d\kappa \qquad (A2)$$

and the volume of the bridging liquid is given by

$$V_b = 2\pi \int_0^\kappa y^2\, g'\, d\kappa - \left[ \begin{array}{l} 2 \times \text{Volume of segment} \\ \text{of spherical particle} \\ \text{obtained by rotating} \\ \text{arc BC around } x \text{ axis.} \end{array} \right] \qquad (A3)$$

Consideration of the geometry of Figure 3 gives $f$, $g$, $h$, and $j$ in terms of $\psi_b$, $\kappa$, and $r_1$:

$$
\begin{aligned}
f &= r_1 (1 - \cos \psi_b) \\
g' &= f/\sin \kappa = \frac{r_1}{\sin \kappa} (1 - \cos \psi_b) \\
h &= r_1 \tan \psi_b \\
j &= r_1 \sin \psi_b + g \cos \kappa \\
\kappa &= \pi/2 - \psi_b - \theta
\end{aligned}
\qquad (A4)
$$

The equation for the area of the bridging liquid can be transformed from the polar coordinate system $(y, \kappa)$ to the rectangular coordinate system $(x, y)$ as follows:

$$A_b = 4\pi \int_0^\kappa y\, g'\, d\kappa = 4\pi \int_0^f y\, \frac{df}{\cos \kappa} \qquad (A5)$$

Since

$$\lim_{\kappa \to 0} df = dx$$

$$A_b = 4\pi \int_0^f y\, \frac{dx}{\cos \kappa}$$

substituting for

$$y = j - (g'^2 - x^2)^{1/2}$$

and

$$\cos \kappa = [1 + x^2 (g'^2 - x^2)^{-1}]^{1/2}$$

we get

$$A_b = 4\pi \int_0^f [j - (g'^2 - x^2)^{1/2}] [1 - x^2 (g'^2 - x^2)^{-1}]^{1/2}\, dx$$

$$= 4\pi g' (j\kappa - f)$$

which in terms of $\psi_b$ and $\theta$ gives

$$A_b = 4\pi r_1^2 \frac{(1 - \cos \psi_b)}{(\cos (\psi_b + \theta))} \{\sin \psi_b + (1 - \cos \psi_b)\cot (\psi_b$$

$$+ \theta)] \left( \frac{\pi}{2} - \psi_b - \theta \right) - (1 - \cos \psi_b)\} \qquad (A6)$$

that is

$$A_b = 4\pi r_1^2 F_1 (\psi_b, \theta)$$

Similarly

$$V_b = 2\pi \int_0^f [j^2 - 2j\, (g'^2 - x^2)^{1/2} + g'^2$$

$$- x^2]\, dx - 2\pi \int_0^f (2r_1 x - x^2)\, dx \qquad (A7)$$

$$= 2\pi \, (ff^2 - ff^2 \cot \kappa - g'^2 j\kappa + fg'^2 - r_1f^2)$$

which in terms of $\psi_b$ and $\theta$ gives

$$V_b = 2\pi r_1^3 \, [(1 - \cos \psi_b) \{\sin \psi_b + (1$$
$$- \cos \psi_b) \cot (\psi_b + \theta)\}^2 - (1 - \cos \psi_b^2)\{\sin \psi_b$$
$$+ (1 + \cos \psi_b) \cot (\psi_b + \theta)\} \cot (\pi/2 - \psi_b - \theta)$$
$$- \left\{ \frac{1 - \cos \psi_b}{\cos (\psi_b + \theta)} \right\}^2 [\sin \psi_b + (1 - \cos \psi_b) \cot (\psi_b$$
$$+ \theta)] \left( \frac{\pi}{2} - \psi_b - \theta \right) + (1$$
$$+ \cos \psi_b) \left\{ \frac{1 - \cos \psi_b}{\cos (\psi_b + \theta)} \right\}^2 - (1 - \cos \psi_b)^2] \quad \text{(A8)}$$

that is

$$V_b = 2\pi r_1^3 \, F_2 \, (\psi_b, \theta)$$

The area of the 12 interface is that of a segment of a sphere and is given by
$$A_{12} = 2\pi r_1 f = 2\pi r_1^2 \, (1 - \cos \psi_b) \quad \text{(A9)}$$
and
$$A_{13} = 4\pi r_1^2 - 2\pi r_1 f$$
$$= 2\pi r_1^2 \, (1 + \cos \psi_b) \quad \text{(A10)}$$

These expressions for $A_b$, $A_{12}$, and $A_{13}$ can be substituted into Equation (10) to determine the free energy of state IV.

## LITERATURE CITED

Albertsson, P. A., *Partition of Cell Particles and Macromolecules*, 2 ed., Wiley-Interscience, New York (1971).

Capes, C. E., "Basic Research in Particle Technology and Some Novel Applications," *Can. J. Chem. Eng.*, 54, 3 (1976).

Doscher, T. M., "Tertiary Oil Recovery," *Chem. Tech.*, 7, 232 (1977).

Erle, M. A., D. C. Dyson, and N. R. Morrow, "Liquid Bridges Between Cylinders, in a Torus, and Between Spheres," *AIChE J.*, 17, 115 (1971).

Henry, J. D., M. E. Prudich, and A. D. Hovarongkura, "Ash Removal from Coal Derived Liquids by Extraction into an Aqueous Phase: Preliminary Feasibility Studies," Final report to ERDA, Grant #90155045, Dept. of Chemical Engineering, West Virginia Univ., Morgantown (1976).

Hotta, K., K. Takeda, and K. Iinoya, "The Capillary Binding Force of a Liquid Bridge," *Powder Tech.*, 10, 231 (1974).

Mayer, R. P., and R. A. Stowe, "Mercury Porosimetry: Filling of Toroidal Void Volume Following Break through between Packed Spheres," *J. Phys. Chem.*, 70, 3867 (1966).

Melrose, J. C., and G. C. Wallick, "Exact Geometrical Parameters for Pendular Ring Fluid," *ibid.*, 71, 3676 (1967).

Melrose, J. C., "Model Calculations for Capillary Condensation," *AIChE J.*, 12, 986 (1966).

Mizrahi, J., and E. Barnea, "The Effects of Solid Additives on the Formation and Separation of Emulsions," *Brit. Chem. Eng.*, 15, 497 (1970).

————, "Systems Consisting of Two Liquid Phases and Solid Particles," *Progr. Heat Mass Trans.*, 6, 717 (1972).

Moody, G. B., ed., *Petroleum Exploration Handbook*, McGraw-Hill, New York (1961).

Princen, H. M., "The Equilibrium Shape of Interfaces, Drops and Bubbles. Rigid and Deformable Particles at Interfaces," *Surface Colloid Sci.*, 2, 1 (1969).

Prudich, M. E., and J. D. Henry, Jr., "The Mechanisms of Transfer of Hydrophobic Coated Matter Particles from a Hydrocarbon to an Aqueous Phase," *AIChE J.*, in press (1978).

Puddington, I. E., and B. D. Sparks, "Spherical Agglomeration Processes," *Min. Sci. Eng.*, 7, 282 (1975).

Rapacchietta, A. V., and A. W. Neumann, "Force and Free-Energy Analyses of Small Particles at Fluid Interfaces. II. Spheres," *J. Colloid Interface Sci.*, 59, 555 (1977).

# An Analytical Study of Ultrafiltration in a Hollow Fiber Artificial Kidney

A theoretical investigation of ultrafiltration through hollow fibers used in artificial kidney applications is presented. The hollow fibers are considered to be cylindrical tubes with ideally selective semipermeable walls which retain cellular particles (red and white cells, platelets) and plasma proteins in the blood perfusing the fibers. In contrast, water and species of low and medium molecular weight can freely permeate the membranes. The assumption is made that secondary flows avoid the formation of concentration boundary layers at the wall. Proper nondimensionalization of the equations for axial and radial transport results in the identification of parameters which are important in the characterization of the ultrafiltration through semipermeable tubes. Perturbation analyses for small values of these parameters lead to sets of differential equations which were solved analytically. These closed form solutions demonstrate the influence of hydraulic conductivity of the fiber walls, geometry, and axial and transmembrane pressure drop on the efficiency of hollow fiber artificial kidneys.

**HEINZ D. PAPENFUSS**

**JOSEPH F. GROSS**

**and**

**STEVEN T. THORSON**

**Department of Chemical Engineering**
**University of Arizona**
**Tucson, Arizona 85721**

## SCOPE

The purpose of an artificial kidney is to replace the function of the human kidney in the case of severe or complete renal failure. This function is to remove certain toxins of low and moderate molecular weight from the blood such as sodium chloride, potassium chloride, urea, creatinine, and uric acid. On the other hand, cellular particles and plasma proteins (macromolecules) should be retained in the blood lumen. Currently, most artificial